

# Graph-based Point Cloud Surface Reconstruction using B-Splines

Stuti Pathak, Rhys G. Evans, Gunther Steenackers, and Rudi Penne

University of Antwerp, Belgium

**Abstract.** Generating continuous surfaces from discrete point cloud data is a fundamental task in several 3D vision applications. Real-world point clouds are inherently noisy due to various technical and environmental factors. Existing data-driven surface reconstruction algorithms rely heavily on ground truth normals or compute approximate normals as an intermediate step. This dependency makes them extremely unreliable for noisy point cloud datasets, even if the availability of ground truth training data is ensured, which is not always the case. B-spline reconstruction techniques provide compact surface representations of point clouds and are especially known for their smoothing properties. However, the complexity of the surfaces approximated using B-splines is directly influenced by the number and location of the spline control points. Existing spline-based modeling methods predict the locations of a fixed number of control points for a given point cloud, which makes it very difficult to match the complexity of its underlying surface. In this work, we develop a Dictionary-Guided Graph Convolutional Network-based surface reconstruction strategy where we simultaneously predict both the location and the number of control points for noisy point cloud data to generate smooth surfaces without the use of any point normals. We compare our reconstruction method with several well-known as well as recent baselines by employing widely-used evaluation metrics, and demonstrate that our method outperforms all of them both qualitatively and quantitatively.

**Keywords:** Point Cloud, Surface Reconstruction, B-Spline, Graph Convolutional Network

## 1 Introduction

Advanced technologies such as LiDAR, photogrammetry and structured light scanning have made the direct acquisition of discrete representations of real-world objects and physical environments around us more accessible and efficient. These 3D representations, formally known as point clouds, are inherently unstructured, contain outliers and are quite noisy due to sensor limitations, multi-view scanning, occlusions and environmental factors. The generation of continuous smooth surface models from these point clouds is extremely crucial for applications in diverse fields like CAD [3], robotics [25], medical imaging [34],

cultural heritage preservation [15], etc. Therefore, the challenging task of reconstructing accurate surfaces from raw point clouds has become an increasingly active area of research in recent years [5, 14, 17].

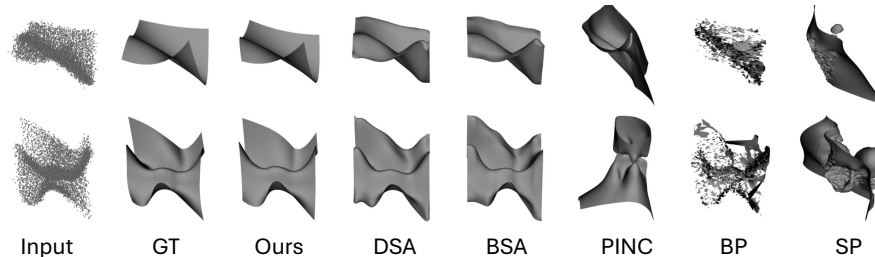


**Fig. 1.** Surface reconstruction of two noisy point clouds using our method and several baselines: Ball-Pivoting (BP) [6], Screened Poisson (SP) [19], Least Square B-spline Surface Approximation (BSA) [27], Differentiable Spline Approximations (DSA) [9], and p-Poisson Surface Reconstruction in Curl-Free Flow (PINC) [26]. This demonstrates our method’s superior visual quality when compared to other approaches.

Surface reconstruction has evolved significantly over the decades, transitioning from classical geometric techniques such as Delaunay triangulation-based methods [2] and Marching cubes [24], to more advanced approaches such as Poisson surface reconstruction [18] and complete or partial machine learning-based techniques [4, 9]. Spline-based surface approximation techniques [27, 31, 35] stand out notably for their capacity to deliver surfaces that are inherently smooth, continuous and accurately represent the underlying geometry of a point cloud. Additionally, because spline surfaces are defined parametrically, they provide a more compact surface representation compared to dense mesh-based models.

Graph Convolutional Networks (GCNs) have emerged as a powerful paradigm in the field of learning-based computer vision, particularly in the context of point cloud data processing. Leveraging graph-based representations, GCNs enable the extraction of meaningful features, capture the spatial dependencies, and learn complex patterns within unstructured point clouds [32]. Over time, several works have explored their relevance for 3D vision tasks such as object recognition [20], segmentation [29], etc. In the context of surface reconstruction, a few works have employed GCNs but have reformulated this task as one of normal estimation [21, 22]. In these approaches, the surface geometry is subsequently derived from the predicted normals.

Regardless of the algorithm employed, surface reconstruction methods often face several persistent challenges, including generation of non-watertight meshes, erroneous and overlapping triangulations, self-occlusions, lack of consistent intermediate normal estimates, high sensitivity to noise as well as to algorithm-specific hyperparameters [17]. While traditional analytical methods often strug-

gle to produce reliable meshes from noisy point clouds, machine learning-based approaches attempt to address this limitation by training on datasets with known ground truth normals or meshes [4, 21, 22]. However, in real-world scenarios, point clouds are typically acquired without access to any ground-truth information. As a result, researchers commonly resort to using synthetic datasets with known ground truth values, or analytically estimated normals as surrogate ground truth, an approach that is itself highly unreliable when dealing with noisy point clouds. In both of the mentioned scenarios, the method generalizability and accuracy for out-of-distribution data reduces significantly. Therefore, there is a need for methods that can directly reconstruct smooth and accurate surfaces from noisy point clouds, without relying on ground-truth normals or their intermediate estimation, while effectively addressing the aforementioned challenges.

A B-spline surface can be completely characterized by its degrees in the two parametric directions, and a grid of control points, whereas other elements such as knot vectors and basis functions can be systematically derived from these primary components. Several spline-based algorithms address the reconstruction task by predicting the location of a fixed number of control points for any given surface [9, 27, 28]. However, the assumption of a fixed number of control points leads to underfitting when this number is insufficient, or overfitting when it exceeds what is necessary to capture the true complexity of the input point cloud (as illustrated in Figure 2). Furthermore, most of these methods work strictly on ordered grid-structured point sets, which makes them unsuitable for unordered point cloud datasets. Hence, a spline-based surface reconstruction method should be able to predict not only the locations of control points but also their appropriate number needed to represent the underlying surface of an unordered point cloud accurately.

In this paper, we address the aforementioned challenges by implementing a graph-based dictionary-guided surface reconstruction technique which fits B-spline surfaces with variable control points to unordered noisy point clouds, without the need of any point normals. Our approach leverages a graph neural network to predict both the locations and the optimal number of control points for a given point cloud. Moreover, we create our own noise-induced point cloud dataset using B-spline modeling. We experiment on both our dataset as well as randomly generated surfaces. We compare our method against several recent and widely-used baselines, both qualitatively (as illustrated in Figure 1) and quantitatively using standard evaluation metrics.

## 2 Related Work

Among the most widely adopted conventional surface reconstruction techniques are the Ball-Pivoting [6] and Screened Poisson [19]. The former simulates a ball rolling over a point cloud, forming triangles whenever it touches three points simultaneously, thereby generating a mesh over the surface. The latter builds on the classic Poisson surface reconstruction [18] by introducing a dualized screening term to improve its geometric fidelity by explicitly incorporating the points of a

point cloud as interpolation constraints. Due to their popularity, these methods have been integrated into various point cloud processing tools such as MeshLab [10]. Although providing accurate surfaces in case of non-noisy and uniformly distributed point clouds, these methods fail miserably when noise comes into play.

Spline-based surface reconstruction methods aim to generate smooth and continuous surfaces from point cloud data by leveraging on B-spline or NURBS (Non-Uniform Rational B-Splines) basis functions. Given a fixed number of control points, least square surface approximation technique using B-splines [27] basically fits spline curves along the two directions of a point cloud. This method adjusts the control points mathematically to best match the spline surface with the input cloud while keeping the surface smooth. Recent papers have shown the applications of spline-based approaches in diverse fields such as industrial manufacturing [31] and areal data analysis [16]. However, inherently, these algorithms not only require the manual tuning of the number control points but also demand a point cloud to be in an ordered grid structure.

With the advent of the machine learning era and the availability of huge point cloud datasets, data-driven surface reconstruction algorithms have emerged as powerful alternatives to traditional methods [14]. A recent paper [9] extends the use of splines, for approximating functions, in differentiable machine learning models by deriving a weak Jacobian for these functions. They demonstrate surface reconstruction from point clouds as an application of their method. [26] proposes a p-Poisson equation-based reconstruction method which learns an approximated signed distance function with the given raw point cloud data. Unlike other machine learning approaches [4, 21, 22], these methods operate solely on the  $xyz$ -coordinates of point clouds, making them suitable baselines for comparison in this study.

All of the methods discussed above are either extremely sensitive to noise or the tuning of their algorithm’s hyperparameters, such as the number of control points for spline-based techniques. In this work, we try to solve the problem of surface reconstruction by modeling the underlying geometry of a noisy point cloud using learnable graph connections and accurate spline fitting. By combining data-driven and analytical techniques, this approach offers an improvement over existing methods that rely solely on one or the other.

### 3 Background

In this section, we present the mathematical definitions of B-spline curves and surfaces which will make the reader familiar with the idea B-spline modeling. Moreover, we highlight the shortcomings of B-spline fitting algorithms.

B-spline, or basis spline, in its simplest form, is a parametric piece-wise polynomial function. A B-spline curve of degree  $k$  with  $n + 1$  control points (CPs)

$\mathbf{P} = \{P_0, P_1, \dots, P_n\}$  is defined as,

$$C(t) = \sum_{i=0}^n N_{i,k}(t) P_i, \quad (1)$$

where,  $N_{i,k}(t)$  are called the basis functions, defined recursively according to the Cox-de Boor formula [11, 12],

$$N_{i,0}(t) = \begin{cases} 1 & \text{if } t_i \leq t < t_{i+1} \\ 0 & \text{otherwise} \end{cases}, \quad (2)$$

$$N_{i,k}(t) = \frac{t - t_i}{t_{i+k} - t_i} N_{i,k-1}(t) + \frac{t_{i+k+1} - t}{t_{i+k+1} - t_{i+1}} N_{i+1,k-1}(t),$$

where,  $t_i$  are called knots defined by a knot vector  $\mathbf{T} = \{t_0, t_1, \dots, t_s\}$ , given  $s = n + k + 1$ .

Essentially, the knots between which a point  $t$  on our curve lies, determine which basis function will affect the shape of our curve at the said point, which eventually determines where and how the CPs influence the curve (Eq. 1). While a uniform knot vector has equally spaced knots, an open knot vector has its first and last knot values repeated  $k + 1$  times [27]. A combination of both, known as the open uniform knot vector, is considered standard in literature, and can be easily computed from the known  $k$  and  $n$  values.

This definition of a B-spline curve when extended in two dimensions leads to a B-spline surface. A B-spline surface is defined as the weighted average of  $(n + 1) \times (m + 1)$  CPs  $P_{ij}$ , where the weights are given by the tensor product of two 1-D basis functions  $N_{i,p}(u)$  and  $N_{j,q}(v)$ ,

$$S(u, v) = \sum_{i=0}^n \sum_{j=0}^m N_{i,p}(u) N_{j,q}(v) P_{ij}, \quad (3)$$

Similar to curves, in this case the two knot vectors  $\mathbf{U}$  and  $\mathbf{V}$  along the two surface parameters  $u$  and  $v$  can be easily pre-computed, and the surface basis functions can then be extracted using Eq. 2. These two surface parameters  $u$  and  $v$  correspond to the parametric directions of the surface.

A key parameter for any B-spline-based reconstruction strategy, which considerably impacts the complexity of the generated surface from a noisy point cloud, is the number of CPs along the two parametric directions (also called the CP grid size). Typically, the values which result in an optimal trade-off between the surface smoothness and approximation quality are determined manually via intuitive trial-and-error. The importance of learning this CP grid size from the data itself is shown in Figure 2, which visualizes the consequences of the inaccurate estimation of these values. Moreover, another disadvantage of these methods lies in the fact that they require the input 3D data to have an ordered grid structure. Motivated by these challenges, our method extracts the correct

CP grid size and the locations of the corresponding CPs from a given unordered non-grid structured point cloud itself.

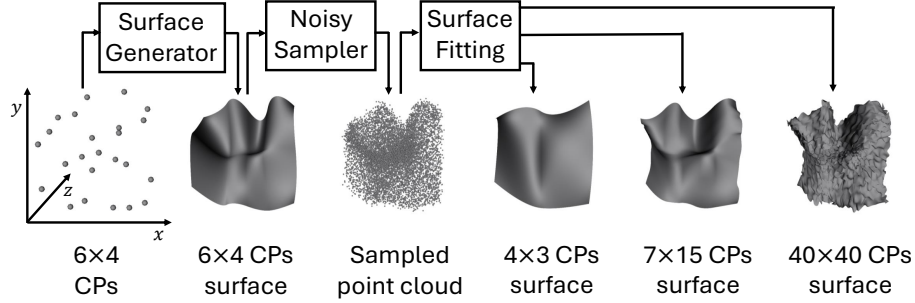


**Fig. 2.** Our dataset creation pipeline for a single point cloud using  $6 \times 4$  CPs spline surface is demonstrated by the first three columns. The remaining columns show the surfaces reconstructed from this point cloud using BSA [27] with fixed CP grid sizes. The underfitting in  $4 \times 3$  CPs surface and the overfitting in  $7 \times 15$  and  $40 \times 40$  CPs surfaces clearly explains the need of variable CP grid size estimation within a reconstruction approach.

## 4 Methodology

### 4.1 Dataset Creation

We generate a point cloud dataset using B-spline modeling as explained in Section 3 with the implementation provided in [7]. Each point cloud instance in our dataset is essentially a noisy version of a sampled B-spline surface, generated using a specific number of CPs in the two spline surface directions. To ensure non-self-intersecting spline surfaces, we first generate a uniformly-spaced  $xy$ -grid for CPs and then superimpose it with some Gaussian noise. However, the  $z$ -coordinates of the CPs vary randomly between a range, which ensures both complex individual surfaces and a comprehensive dataset. We then define the spline degrees and compute two open uniform knot vectors eventually used for B-Spline basis functions generation. The said CP grid and the basis functions generated are used to simulate a B-spline surface. This surface is first randomly sampled and then per point Gaussian noise is added. The first three figures of Figure 2 visually demonstrate the generated CPs (with grid size  $6 \times 4$ ), subsequent B-spline surface and the noisy sampled point cloud respectively, as an example of this data creation method. Several random samples with one CP grid size are generated. This exact procedure is repeated for several other CP grid sizes to generate a point cloud dataset with underlying B-spline surfaces of varying grid sizes. To train our model, we generate two datasets using the described

method: one containing point clouds from two CP grid sizes, and another with three. By adjusting the input parameters of this generation process, users can tailor the complexity of the training datasets to suit their requirements.

As mentioned before, in this work we aim to predict both the number as well as the location of CPs for each test sample. This way we overcome the widely-adopted fixed CP grid size approach. The fact that the ground truth CP grid sizes are different for different instances of our dataset, makes our dataset unsuitable for a GCN model. To overcome this, we take advantage of the concept of zero-padding from machine learning-assisted 3D vision literature. Suppose, a sample from the dataset has a CP grid size of  $i \times j$  then its CP grid matrix will be of size  $i \times j \times 3$ . We expand this matrix to a larger size of  $I \times J \times 3$  such that all the new elements introduced to the original matrix are padded with zeros. Here,  $I$  and  $J$  are greater than the largest point cloud CP grid size in the dataset. We do this for all the samples. Additionally, to ensure better generalization after training, we randomly remove several points from each point cloud and shuffle the order of the remaining points. This enables our model to operate effectively on unordered point clouds, unlike traditional spline approximation methods that rely on ordered and gridded point sets.

## 4.2 Graph-based Surface Reconstruction using B-Splines

Figure 3 illustrates our model architecture. The pipeline integrates graph-based feature extraction, a learnable dictionary module, and a B-spline surface generator to reconstruct smooth surfaces from noisy point clouds. The process begins by feeding a noisy point cloud into several GCN layers, which extract local features. These features are aggregated into a global representation through pooling operations. This global feature vector is then refined via a dictionary-guided mechanism. The learnable dictionary captures recurring patterns between the ground truth CP values and the input cloud during training, allowing the model to learn useful priors. At inference time, these learned priors help guide accurate prediction of CPs. Finally, these CPs act as compact surface representations of the input point cloud and are used by the B-spline surface generator to reconstruct the final surface.

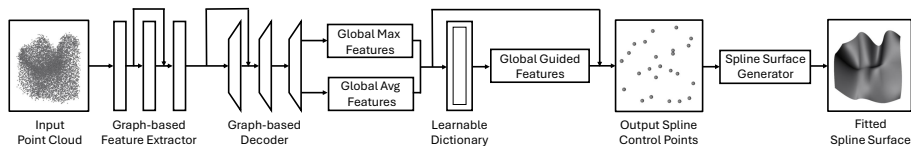


**Fig. 3.** Graph-based Surface Reconstruction using B-Splines architecture.

We employ a weighted Mean Squared Error (MSE) loss function and Adam optimizer to backpropagate the error between the predicted and the ground

truth CPs. This weighted loss function gives higher importance to accurately predicting the zero-padded values in the output CPs (as discussed in Section 4.1). This facilitates easy CP grid extraction later. We also incorporate skip connections between the GCN layers to preserve local structure information along the network. Our model trains on an NVIDIA GeForce RTX 4090 24GB GPU.

## 5 Experiments

We conduct three sets of experiments: (1) training and testing on our own dataset with two CP grid sizes  $[3 \times 4, 5 \times 6]$  containing 6000 noisy point clouds, (2) training and testing on our own dataset with three CP grid sizes  $[3 \times 4, 5 \times 6, 3 \times 6]$  containing 9000 noisy point clouds, and (3) evaluating the generalization abilities of our model, pre-trained on our own dataset, on random surfaces. To generate these random surfaces we use the Blender software [8] in which we manipulate gridded surfaces with geometry nodes and apply texture nodes to the normal  $z$ -axis of the surface. Changing the hyperparameters of these texture nodes creates complex topologies with random surface peaks and troughs.

We compare our method against several widely-used and recently proposed surface reconstruction techniques that do not rely on normal estimation at any stage of their pipeline: (1) Ball-Pivoting (BP) [6], (2) Screened Poisson (SP) [19], (3) Least Square B-spline Surface Approximation (BSA) [27], (4) Differentiable Spline Approximations (DSA) [9], and (5) p-Poisson Surface Reconstruction in Curl-Free Flow (PINC) [26]. We preprocess the unordered point clouds in our dataset by applying gridding and ordering techniques (using Python’s scientific libraries) for methods (3) and (4). This step is necessary to make the data compatible with these methods, which, as discussed in Section 3, are inherently unable to operate on unordered point sets.

To quantitatively evaluate the accuracy of our method we adopt three error metrics which basically measure the similarity between the original non-noisy point cloud and the point cloud randomly sampled from the generated surface by our method and the mentioned baselines. Lower values of these metrics indicate greater similarity between the two point clouds, reflecting more accurate surface reconstruction. We provide a brief description of these metrics along with their significance below:

Earth Mover’s Distance (EMD) is universally-adopted as not just an evaluation metric but also an optimization strategy for several point cloud processing techniques [13, 23]. It basically tries to find the best mapping function from one point cloud to another. It is recognized for delivering more reliable visual quality and offering a better intuitive measure of similarity between two point clouds when compared to the standard Chamfer Distance (CD) [1, 23, 33].

Normal Consistency (NC) measures the angular alignment between the surface normals of corresponding points in two point clouds, capturing local geometric similarity. To compute this metric each point in one point cloud is mapped to

its nearest neighbor in the other. This metric emphasizes on local smoothness and is commonly used in surface reconstruction and normal estimation tasks [4, 22].

Density-aware Chamfer Distance (DCD) is a recently proposed similarity metric [33] that accounts for both the density distribution and fine structural details of the input point cloud. Its development is motivated by the limitations of the standard CD, which tends to perform poorly on datasets with outliers and noise [30]. DCD is derived from the original CD, but has a higher tolerance to outliers through an approximation of Taylor expansion.

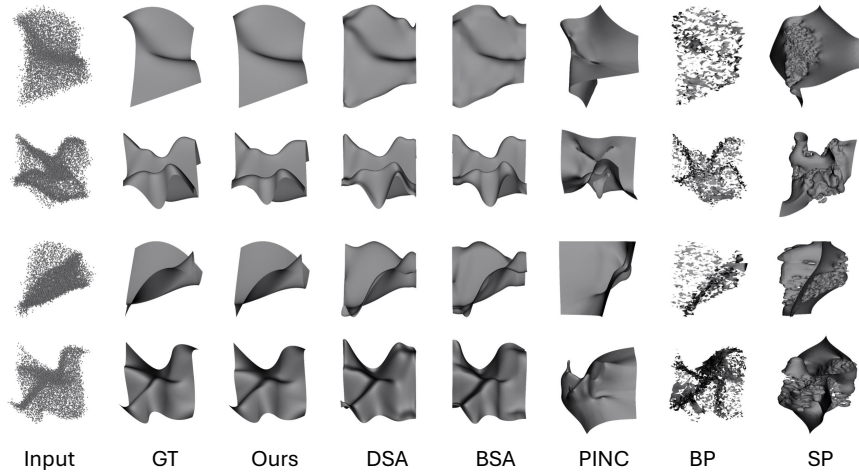


**Fig. 4.** Surface reconstruction visualizations of four different point clouds from our dataset using our method and the other baselines. This showcases the visual superiority of our method over others.

## 6 Results

In this section, we present a comprehensive quantitative and qualitative evaluation of our method in comparison to the aforementioned baselines. Table 1 reports the average values of the three performance metrics NC, DCD, and EMD across two point cloud testing datasets with varying CP grid sizes. The results clearly demonstrate that our method consistently outperforms all the baselines, producing surfaces that are most similar to the ground truth (as discussed in Section 5). These quantitative results are further corroborated by qualitative visualizations shown in Figure 4, which illustrate the superior surface reconstruction quality of our approach visualized for four input point clouds. In particular, while BP is incapable of producing watertight surfaces, SP and PINC overfit the noisy point cloud to a huge extent providing less to no smoothening over the

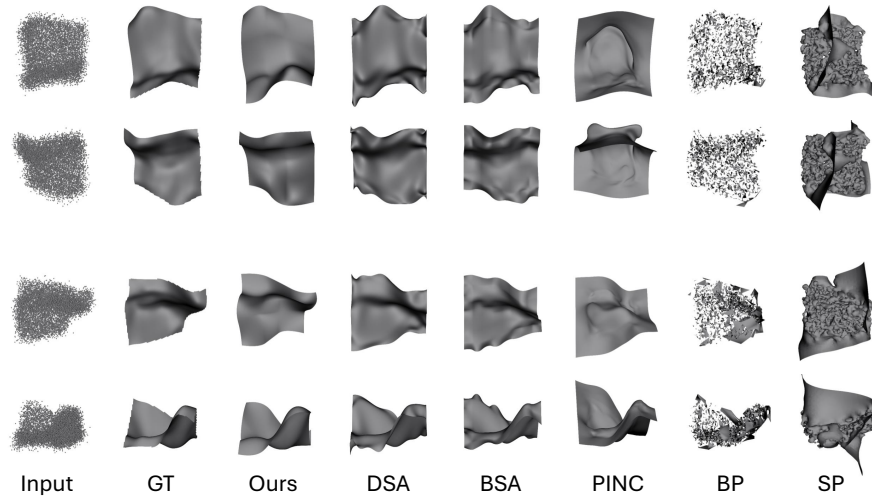


**Fig. 5.** Surface reconstruction by our method and the other baselines experimented on two random surfaces generated using Blender [8] visualized from two different view angles. The first two rows correspond to the first surface, while the remaining two the second. This visualization highlights our method’s ability to generalize to arbitrary surfaces.

noise. Although BSA and DSA reconstruct surfaces that somewhat resemble the ground truth, their outputs also tend to overfit to the noisy input data. This behavior could be attributed to the fixed CP grid size used in their algorithms.

Since point clouds in general vary in complexity and size, the dataset creation method described in Section 4.1 allows for the generation of customized training datasets tailored to specific user requirements. Based on the complexity of this training data even the model’s complexity can be adjusted to ensure optimal performance.

Additionally, we experiment on some random surfaces generated by Blender (as mentioned in Section 5) as shown in Figure 5. All the baselines show the same trend as observed in the previous experiments. Our model, once again, closely resembles the ground truth and gives the best visual results.

To further demonstrate the effectiveness of our approach, we include a video in the supplementary material showcasing 360° visualizations of all the figures in our paper, excluding Figure 3, to help readers better appreciate the accuracy and visual quality of our method as compared to other baselines.

	2 CP grid sizes dataset			3 CP grid sizes dataset		
	DCD ( $\downarrow$ )	NC ( $\downarrow$ )	EMD ( $\downarrow$ )	DCD ( $\downarrow$ )	NC ( $\downarrow$ )	EMD ( $\downarrow$ )
BP	80.9	25.9	3.3	80.6	25.9	3.4
SP	77.0	21.2	2.8	77.7	20.9	2.9
BS	52.2	10.5	2.6	53.4	11.0	2.6
DSE	52.4	10.4	3.2	52.9	10.4	3.1
PINC	93.7	32.3	5.9	93.0	32.9	5.6
Ours	<b>51.8</b>	<b>8.7</b>	<b>1.2</b>	<b>46.9</b>	<b>8.1</b>	<b>1.2</b>

**Table 1.** Quantitative comparison of our method against various baselines on two test datasets (with varying CP grid sizes) using the average values of three error metrics: Earth Mover’s Distance (EMD), Normal Consistency (NC), and Density-aware Chamfer Distance (DCD). All values are reported in units of  $\times 10^{-2}$ . Lower metric values indicate better surface reconstruction, with our method achieving the best performance.

## 7 Conclusion

Surface reconstruction from noisy point cloud data hails as one of the most challenging yet essential tasks in the computer vision community. In this paper, we try to address several drawbacks of existing reconstruction techniques such as the use of either ground truth normals or their inconsistent intermediate estimation in learning-based techniques, and fixed control points approach in case of spline-based reconstruction algorithms. We do this by leveraging a graph-based dictionary-guided learning strategy and B-spline surface fitting to obtain compact surface representations of noisy input point clouds without using any point normals. We evaluate our results based on three error metrics and compare them with several baselines. We also provide visualizations of the reconstructions obtained by our method and the other baselines used. Our method demonstrates superior performance in both the quantitative metrics and the visual quality of the reconstructed surfaces by introducing the concept of variable spline control points and eliminating the reliance on point normals.

## References

1. P. Achlioptas, O. Diamanti, I. Mitliagkas, and L. Guibas. Learning representations and generative models for 3d point clouds. In *International conference on machine learning*, pages 40–49. PMLR, 2018.
2. N. Amenta and M. Bern. Surface reconstruction by voronoi filtering. In *Proceedings of the fourteenth annual symposium on Computational geometry*, pages 39–48, 1998.
3. S. Azernikov and A. Fischer. Efficient surface reconstruction method for distributed cad. *Computer-Aided Design*, 36(9):799–808, 2004.

4. Y. Ben-Shabat and S. Gould. Deepfit: 3d surface fitting via neural network weighted least squares. In *Computer Vision–ECCV 2020: 16th European Conference, Glasgow, UK, August 23–28, 2020, Proceedings, Part I 16*, pages 20–34. Springer, 2020.
5. M. Berger, A. Tagliasacchi, L. M. Seversky, P. Alliez, G. Guennebaud, J. A. Levine, A. Sharf, and C. T. Silva. A survey of surface reconstruction from point clouds. In *Computer graphics forum*, volume 36, pages 301–329. Wiley Online Library, 2017.
6. F. Bernardini, J. Mittleman, H. Rushmeier, C. Silva, and G. Taubin. The ball-pivoting algorithm for surface reconstruction. *IEEE transactions on visualization and computer graphics*, 5(4):349–359, 2002.
7. O. R. Bingol and A. Krishnamurthy. NURBS-Python: An open-source object-oriented NURBS modeling framework in Python. *SoftwareX*, 9:85–94, 2019.
8. Blender Online Community. Blender - a 3d modelling and rendering package. <https://www.blender.org>, 2025. Version 4.2 LTS.
9. M. Cho, A. Balu, A. Joshi, A. Deva Prasad, B. Khara, S. Sarkar, B. Ganapathysubramanian, A. Krishnamurthy, and C. Hegde. Differentiable spline approximations. *Advances in neural information processing systems*, 34:20270–20282, 2021.
10. P. Cignoni, M. Callieri, M. Corsini, M. Dellepiane, F. Ganovelli, and G. Ranzuglia. MeshLab: an Open-Source Mesh Processing Tool. In V. Scarano, R. D. Chiara, and U. Erra, editors, *Eurographics Italian Chapter Conference*. The Eurographics Association, 2008.
11. M. G. Cox. The numerical evaluation of b-splines. *IMA Journal of Applied mathematics*, 10(2):134–149, 1972.
12. C. De Boor. On calculating with B-splines. *Journal of Approximation theory*, 6(1):50–62, 1972.
13. H. Fan, H. Su, and L. J. Guibas. A point set generation network for 3d object reconstruction from a single image. In *Proceedings of the IEEE conference on computer vision and pattern recognition*, pages 605–613, 2017.
14. A. Farschian, M. Götz, G. Cavallaro, C. Debus, M. Nießner, J. A. Benediktsson, and A. Streit. Deep-learning-based 3-d surface reconstruction—a survey. *Proceedings of the IEEE*, 111(11):1464–1501, 2023.
15. L. Gomes, O. R. P. Bellon, and L. Silva. 3d reconstruction methods for digital preservation of cultural heritage: A survey. *Pattern Recognition Letters*, 50:3–14, 2014.
16. C. Harmening and H. Neuner. Choosing the optimal number of B-spline control points (Part 2: Approximation of surfaces and applications). *Journal of Applied Geodesy*, 11(1):43–52, 2017.
17. Z. Huang, Y. Wen, Z. Wang, J. Ren, and K. Jia. Surface reconstruction from point clouds: A survey and a benchmark. *IEEE transactions on pattern analysis and machine intelligence*, 2024.
18. M. Kazhdan, M. Bolitho, and H. Hoppe. Poisson surface reconstruction. In *Proceedings of the fourth Eurographics symposium on Geometry processing*, volume 7, 2006.
19. M. Kazhdan and H. Hoppe. Screened poisson surface reconstruction. *ACM Transactions on Graphics (ToG)*, 32(3):1–13, 2013.
20. L. Landrieu and M. Simonovsky. Large-scale point cloud semantic segmentation with superpoint graphs. In *Proceedings of the IEEE conference on computer vision and pattern recognition*, pages 4558–4567, 2018.
21. J. E. Lenssen, C. Osendorfer, and J. Masci. Deep iterative surface normal estimation. In *Proceedings of the IEEE/CVF conference on computer vision and pattern recognition*, pages 11247–11256, 2020.

22. K. Li, M. Zhao, H. Wu, D.-M. Yan, Z. Shen, F.-Y. Wang, and G. Xiong. Graphfit: Learning multi-scale graph-convolutional representation for point cloud normal estimation. In *European Conference on Computer Vision*, pages 651–667. Springer, 2022.
23. M. Liu, L. Sheng, S. Yang, J. Shao, and S.-M. Hu. Morphing and sampling network for dense point cloud completion. In *Proceedings of the AAAI conference on artificial intelligence*, volume 34, pages 11596–11603, 2020.
24. W. E. Lorensen and H. E. Cline. Marching cubes: A high resolution 3d surface construction algorithm. In *Seminal graphics: pioneering efforts that shaped the field*, pages 347–353. 1998.
25. P. Mittendorf and G. Cheng. 3d surface reconstruction for robotic body parts with artificial skins. In *2012 IEEE/RSJ International Conference on Intelligent Robots and Systems*, pages 4505–4510. IEEE, 2012.
26. Y. Park, T. Lee, J. Hahn, and M. Kang.  $p$ -poisson surface reconstruction in curl-free flow from point clouds. *Advances in Neural Information Processing Systems*, 36:60077–60098, 2023.
27. L. PIEQL and W. TILLER. The nurbs book (monographs in visual communication), 1997.
28. G. Sharma, D. Liu, S. Maji, E. Kalogerakis, S. Chaudhuri, and R. Měch. ParSeNet: A parametric surface fitting network for 3D point clouds. In *Computer Vision—ECCV 2020: 16th European Conference, Glasgow, UK, August 23–28, 2020, Proceedings, Part VII 16*, pages 261–276. Springer, 2020.
29. W. Shi and R. Rajkumar. Point-gnn: Graph neural network for 3d object detection in a point cloud. In *Proceedings of the IEEE/CVF conference on computer vision and pattern recognition*, pages 1711–1719, 2020.
30. M. Tatarchenko, S. R. Richter, R. Ranftl, Z. Li, V. Koltun, and T. Brox. What do single-view 3d reconstruction networks learn? In *Proceedings of the IEEE/CVF conference on computer vision and pattern recognition*, pages 3405–3414, 2019.
31. G. Wang, H. Liu, J. Luo, L. Mou, and H. Pu. Reconstruction of smooth skin surface based on arbitrary distributed sparse point clouds. *IEEE Transactions on Industrial Informatics*, 19(11):10663–10673, 2023.
32. Y. Wang, Y. Sun, Z. Liu, S. E. Sarma, M. M. Bronstein, and J. M. Solomon. Dynamic graph CNN for learning on point clouds. *ACM Transactions on Graphics (tog)*, 38(5):1–12, 2019.
33. T. Wu, L. Pan, J. Zhang, T. Wang, Z. Liu, and D. Lin. Density-aware chamfer distance as a comprehensive metric for point cloud completion. *arXiv preprint arXiv:2111.12702*, 2021.
34. Z. Xiong, M. K. Stiles, Y. Yao, R. Shi, A. Nalar, J. Hawson, G. Lee, and J. Zhao. Automatic 3d surface reconstruction of the left atrium from clinically mapped point clouds using convolutional neural networks. *Frontiers in Physiology*, 13:880260, 2022.
35. S. Yuwen, G. Dongming, J. Zhenyuan, and L. Weijun. B-spline surface reconstruction and direct slicing from point clouds. *The International Journal of Advanced Manufacturing Technology*, 27:918–924, 2006.